Clouds and the Earth's Radiant Energy System (CERES)

Validation Document

Imager Cloud-Top Heights and

Imager Cloud-Base Heights

(Subsystem 4.2)

Patrick Minnis[1]
William L. Smith, Jr.[1]
Xiquan Dong[2]
Yan Chen[3]
Bruce A. Wielicki[1]
Bryan A. Baum[1]

[1]Atmospheric Sciences Division
NASA Langley Research Center
Hampton, VA 23681-0001

[2]Department of Meteorology
University of Utah
Salt Lake City, UT 84112

[3]SAIC
Hampton, VA 23666

August 2000

4.2.1 Introduction

4.2.1.1 Measurement and Science Objectives

This document describes a strategy for addressing the verification of cloud-top and base altitudes and cloud overlapping determined from EOS imager data for CERES. The methodologies for this task have been detailed by Baum et al. (1995), Minnis et al. (1995;1999a,b), and Trepte et al. (1999). The CERES cloud retrieval algorithms were developed using data from the Advanced Very High Resolution Radiometer (AVHRR, 1.1 or 4-km resolution at nadir), the High Resolution Infrared Radiometer Sounder (HIRS, 17.4-km resolution at nadir), various geostationary platforms such as the Geostationary Operational Environmental Satellite (GOES; 1-km visible, 4-km infrared), and, since 1998, the Tropical Rainfall Measurement Mission (TRMM) Visible-Infrared Radiometer (VIRS, 2-km resolution). Additional development will occur when new spectral channels are available from the Moderate Resolution Imaging Spectroradiometer (MODIS; 0.25, 05. and 1-km resolution) on the EOS satellites. While the CERES cloud height algorithms were designed to function with input from any imager dataset, a number of questions remain as to how consistent the cloud retrievals are between the various imagers. Besides the differences in spectral channels between imagers, there are also differences in pixel resolution and time and angular sampling. In the following sections, a number of strategies are outlined, in order of priority, for verifying the vertical cloud boundaries or cloud heights. Examples of preliminary validations of the CERES analysis of VIRS data are shown.

4.2.2.2 Missions

The first launch of the CERES instrument was on the TRMM in late 1997. Operational analysis of CERES TRMM data began in January 1998. Another CERES package was launched on the EOS-AM-1 platform, Terra, in late 1999. It will be followed by another on the EOS-PM-1, Aqua. Follow-on missions to TRMM and EOS-AM and EOS-PM are currently planned. The CERES algorithms will be applied to data from MODIS on both Terra and Aqua.

4.2.2.3 Science data products

The cloud properties generated from imager data in CERES Subsystem 4.1, 4.2 and 4.3 will be convolved with CERES broadband radiometric data and saved in the CERES SSF product. The validation approaches outlined for the CERES Subsystem 4.1 (Minnis et al. 2000a), clear-sky determination and cloud detection, serve as the basis for much of the validation of the other CERES cloud products including those discussed in this section. Thus, the discussion in the 4.1 Validation Plan will be referenced when appropriate and repeated only when necessary.

4.2.2 Validation Criterion

4.2.2.1 Overall approach

The validation strategy involves several key elements. The first element is visual quality control; the results, when displayed, should be consistent with a visual interpretation of the imagery and lack spatial discontinuities that are obvious artifacts of the correlative input data. The second approach is to ensure that the retrieved cloud properties are consistent globally for both daytime and nighttime conditions and are reasonable in a climatological context. Finally, assuming that the clear-sky and cloud properties are consistent and reasonable on a global scale, the results should compare well with independent observations from ground-, air-, and other satellite-based observations.

The CERES cloud algorithms include a variety of input data that are used to predict clear-sky radiances, set thresholds, and retrieve parameters via comparison with theoretical models. The primary technique for determining cloud-top height is to first estimate the cloud temperature and then relate that temperature to altitude or pressure from a vertical profile of atmospheric temperature. Currently, the ECMWF analyses provide those profiles for the algorithms, except over ocean where a single lapse rate anchored to the sea surface temperature is used conditionally for the first 2 km above the surface. This modification eliminates much of the uncertainty arising from boundary layer inversions that are not captured in many numerical weather analyses. Thus, there are two components that must be considered when evaluating the results, the cloud temperature and the temperature profile. If both are correct, then the derived altitudes should also be correct.

The inspection of raw imagery and the corresponding retrievals, especially during the initial processing stages, is useful for detecting the most obvious problems. Because it is a subjective process, inspection is only a qualitative validation, but extremely useful. Some of the identified problems may be easily resolved, while others may be indicative of more subtle algorithm implementation errors. Data from each imager have idiosyncrasies that require some iterative analysis to understand. Differences in boundaries between ECMWF grids, CERES grids, and CERES analysis tiles (arrays of pixels analyzed together) may also introduce some artifacts that can be easily detected visually. Software changes will be developed and implemented to account for those idiosyncrasies and artifacts when possible.

Several methods are available for implementing steps to address the second key element. Proof of consistency may be found, for example, from inspection of global maps of derived cloud heights, from comparison with previous results for some specified time period, or by comparison with other global clear-sky and cloud products such as the International Satellite Cloud Climatology Project (ISCCP), surface observation climatologies, or Clouds from AVHRR (CLAVR). Global, gridded clear-sky and cloud products are generated during processing to facilitate such comparisons. The global comparisons provide a measure of reasonableness while also permitting the detection of some possible large-scale, diurnal, or input problems. This type of approach led to the implementation of the boundary layer lapse rate method over ocean regions.

The most quantitative method for validating the vertical cloud boundaries is accomplished by comparisons with independent observations. Differences between the satellite-retrieved cloud heights and airborne- or ground-based observations will be performed over a long time period for a number of regions, as discussed later in this document.

4.2.2.2 Sampling requirements and trade-offs

The satellite cloud height retrievals can be organized by cloud type or thickness over the globe because cloud types are often spatially dependent and cloud thickness affects the determination of cloud temperature. The following categories are defined to facilitate the assessments through visual, global, and:

a. Cloud types: low, middle, high, and multiple layer

b. Surface types: ocean (Tropics, midlatitude, and polar), vegetated land (Tropics and midlatitude), non-vegetated land (deserts, other), mountains, snow-covered land (midlatitude and polar), ice-covered water

c. Seasons: summer, winter, transition

d. Day/night: Separate categories are not defined for twilight or sunglint conditions. For twilight conditions (82° < SZA < 88°), the nighttime algorithm is applied with some additional visible-channel reflectance checks. Sunglint cannot be ignored for overpasses over water and deserts.

This set of categories yields a total of 4*11*3*2= 264 conditions. To obtain a complete quantitative assessment (i.e., direct comparisons with independent, ground-truth observations), it would probably be necessary to have on the order of 100 independent samples for each of the conditions, or 100*264=26,400 samples. It is unlikely that this number of samples will be obtainable for all of the different categories. Additionally, other factors that affect cloud height retrievals, like cloud cell size or aspect ratios, are not considered in these categories. Thus, a complete assessment of all conditions would require an even greater number of samples than the estimate above.

A set of 30 regions has been selected to facilitate the validation of cloud properties for the conditions noted above. These regions are listed in Table 2 of Minnis et al. (2000a). Pixel-level results from the CERES cloud retrieval algorithm as well as the accompanying input data are saved for each satellite swath including one of these 30 sites. The results are processed into imagery used for visual validation and are also averaged over particular scales to match available surface and aircraft observations.

4.2.2.3 Measures of Success

The CERES cloud retrieval algorithms to discern whether each satellite imager (i.e., AVHRR, MODIS, VIRS) pixel contains none, one, or multiple cloud layers. The validation is considered complete when the uncertainties have been determined to be within the accuracies shown in Table 1 over all major surface types for the full range of applicable viewing angles at all times of day.

The all-purpose algorithm for cloud-top height detection is the Layered Bispectral Threshold Method (LBTM; Minnis et al. 1995b). The LBTM approach works with any imager data having at least a visible (~0.65 µm) channel and an infrared (~11 µm) channel. The LBTM is used as a initial height determinant that is later refined by the Visible Infrared Solar-infrared Split-window Technique (VISST) during daytime and by the Solar-infrared Infrared Split-window Technique (SIST) at night. A CO_2 slicing method will eventually be used for mid- to high-level clouds employing MODIS channels within the15-micron CO_2 band. Detection of overlapped clouds is still an experimental process and will not be subject to ant strict uncertainty guidelines. Nevertheless, the validation process will be used to determine the uncertainties in the cloud overlap determinations. The overall goal of the cloud height validation is to obtain the desired accuracies shown in Table 1.

Table 1: Current and desired accuracies for cloud-top and cloud-base pressure retrievals.

Parameter	Current Accuracy (hPa)	Desired Accuracy (hPa)
High cloud-top pressure: a. LBTM/VISST/SIST b. CO_2 slicing	a. 50 b. 50	a. 25 b. 25
High cloud-base pressure: a. LBTM/VISST/SIST	a. 70	a. 50
Mid-level cloud-top pressure a. LBTM/VISST/SIST b. CO_2 slicing	a. 50 b. 50	a. 25 b. 25
Mid-level cloud-base pressure a. LBTM/VISST/SIST	a. 50	a. 50
Low cloud-top pressure: a. LBTM/VISST/SIST b. Spatial coherence	a. 30 b. 50	a. 25 b. 25
Low cloud-base pressure: a. LBTM/VISST/SIST	a. 25	a. 25

4.2.3 Pre- and Postulant Algorithm Test/Development Activities

4.2.3.1 Visual quality control

The first step in the process of verification is to make certain that the cloud properties in a given scene are consistent with the imagery and do not show any artifacts related to input fields and surface type boundaries. These visual procedures have been performed for the past 3 years by the CERES Cloud Working Group are consistent on a global scale for both daytime and nighttime retrievals. Figure 1 shows an example of the imagery used to perform the visual cloud height consistency analyses. The 3-channel false color VIRS swath in the upper left-hand corner shows an low clouds in the right half of the swath and a mixture of thin cirrus (pink) and thicker mid-to-high clouds on the left side. The cloud temperatures vary from 285 K on the right to as low as 225K on the right. The resulting cloud heights range from 1 - 2 km on the right and from 7 to 11 km on the right. Cloud pressure is relatively uniform over the low stratocumulus clouds and varies by a little

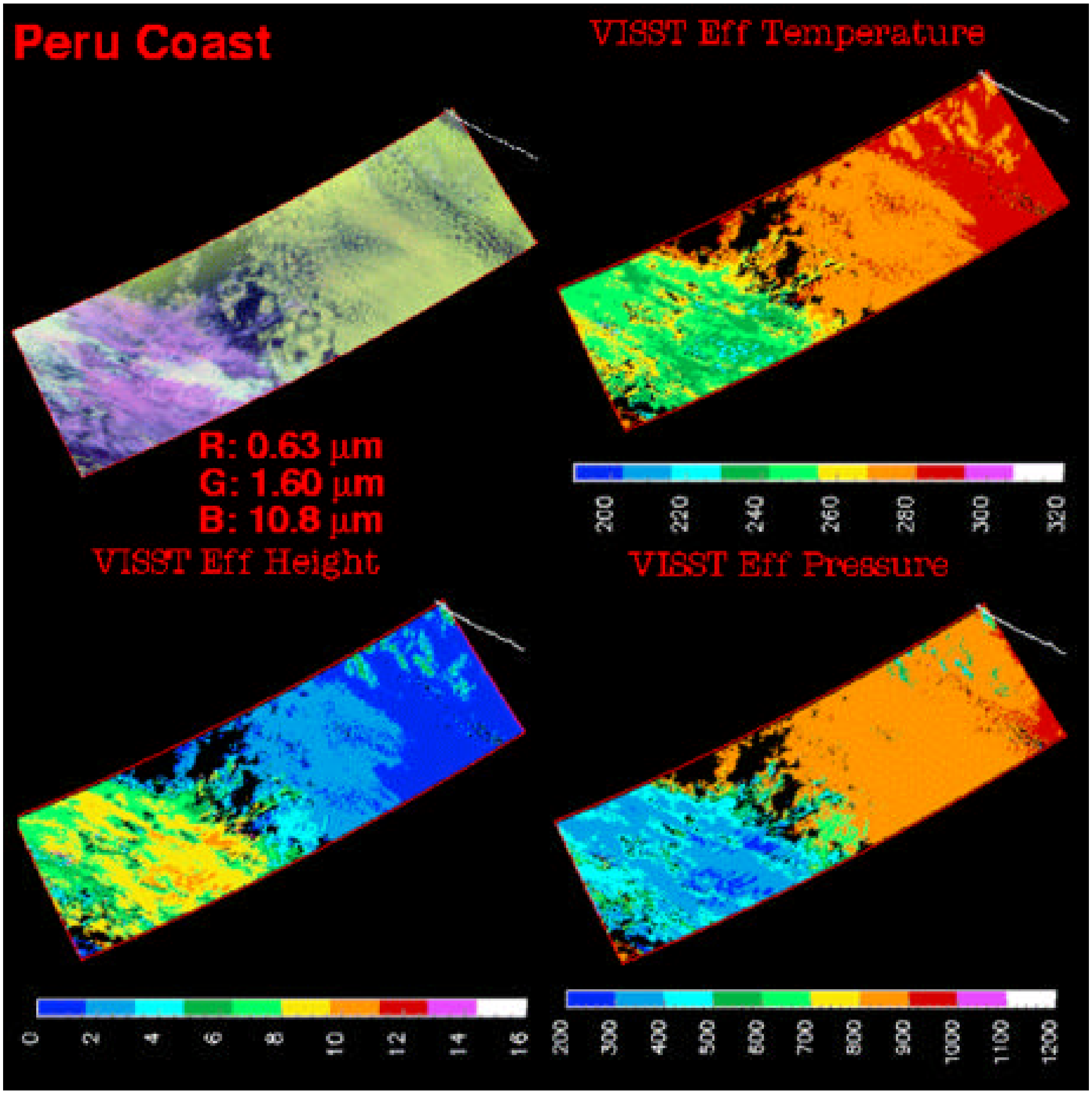

Figure 1. VIRS multispectral imagery and CERES-derived cloud parameters off Peruvian coast 1200 UTC, 12 June 1998.

more than 200 hPa on the right side of the image. No artificial lines or discontinuities are evident in the imagery. Discontinuities across surface type boundaries for similar cloud types are one example of problems that could be detected through visual inspection. Images like those in Figure 1 have been created and examined for many VIRS cases. Similar visual examination will be performed for the MODIS results and continued for VIRS. When distinct problems appear in the imagery, then the input data are examined to track down the source of the apparent problem. By following this procedure, it is possible to correct algorithmic and input defects and also explain the occurrence of unusual phenomena in the data.

.

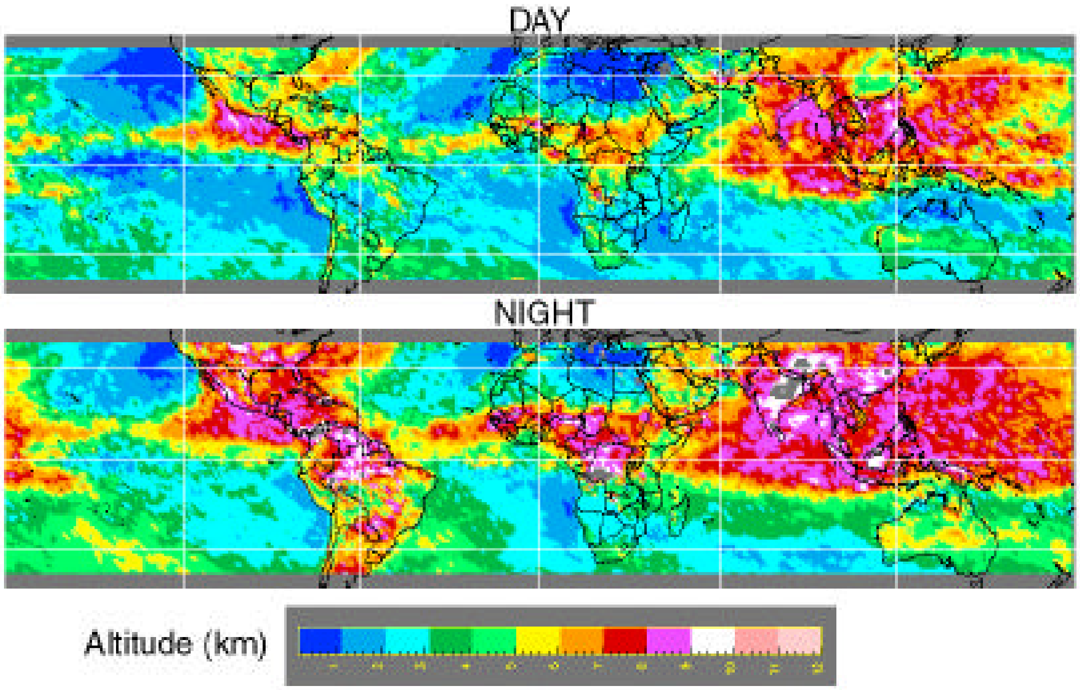

Figure 2. Mean cloud-top heights derived from VIRS with a preliminary CERES VISST (daytime) and SIST (nighttime) for July 1998.

4.2.3.2 Global, day/night, and angular consistency

Monthly mean plots can be used to obtain a qualitative validation of the reasonableness of the derived cloud height fields. For example, Figure 2 shows the results from a preliminary version of the CERES cloud algorithms applied to July 1998 data. The results all look reasonable relative to known features of global cloud climatology. For example, the Intertropical Convergence Zones over the Pacific and Atlantic, marked by areas of cloud heights above 6 km, are in their proper locations, while the regions of marine stratocumulus west of California, Peru, South Africa and north Africa are quire distinct and show height patterns consistent with the climatology of increasing cloud height west of the coasts. The cloud heights are greater at night over almost all regions. Convective development over land during the afternoon is common while marine stratocumulus clouds tend to rise and thicken during the night. However, the magnitude of the changes seen here are larger than expected. Some of this effect is probably due to the different algorithms used for night analyses as discussed later. It is clear from even a cursory examination of Figure 2 and similar figures, however, that such plots are extremely valuable for gross verification of the resulting cloud heights. These types of plots are being produced and examined by the CERES Cloud Working Group to determine the overall reasonableness of the VIRS results. When MODIS results become available, comparisons of the VIRS and MODIS products will also aid the validation process.

Ideally, cloud heights should be invariant with viewing angles, but may change systematically with solar zenith angles if there is a diurnal cycle in cloud altitude. To determine if the algorithm derives cloud heights that are sensitive to the viewing angles, cloud-top altitude is averaged over the

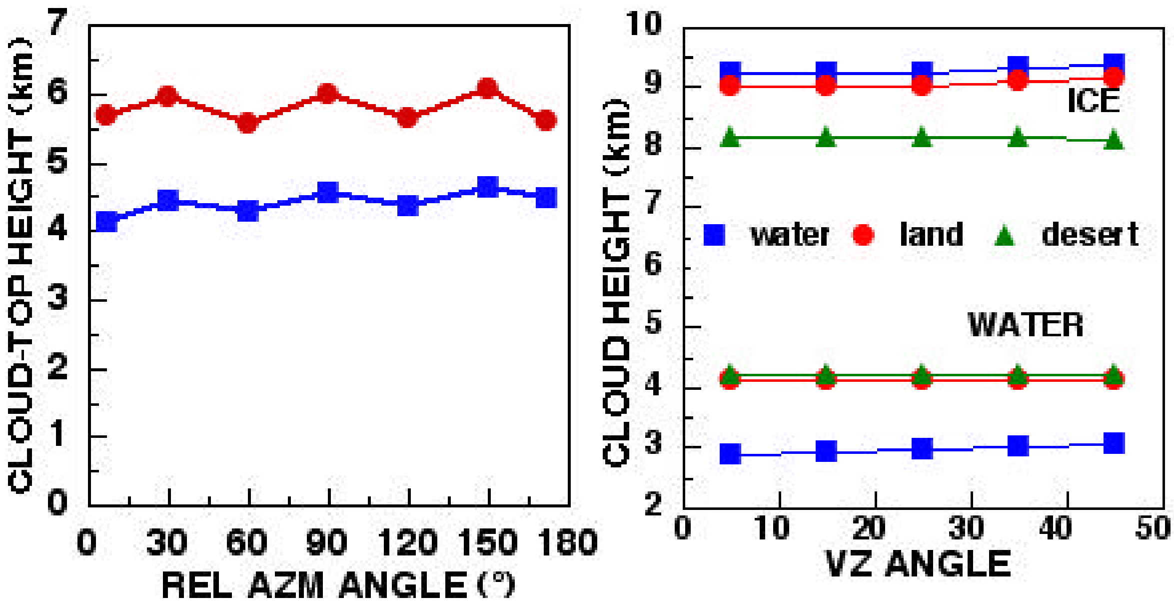

Figure 3. Angular dependence of January 1998 mean daytime cloud heights from VIRS derived with the CERES VISST.

range of angles and scene types. Figure 3 shows the mean cloud heights from a preliminary version of the CERES algorithm applied to VIRS data taken during January 1998. A slight increase in cloud height with both relative azimuth (REL AZM) angle and viewing zenith (VZ) angle is apparent over water surfaces for both ice and water clouds. Systematic variation of cloud height over land and desert is negligible, except for a slight increase with VZ angle for ice clouds over land. The REL AZM dependence over water is probably due to sun glint effects, but the source of the VZ variations is not immediately evident. The imager sampling patterns should be considered in any assessment of averaged quantities because some variations may arise from uneven sampling. For example, VIRS may sample a tropical region at nearly each local hour during a month, but may only view subtropical and midlatitude areas during only few local hours. Additionally, regions near the highest latitude of the VIRS view (~38°) are only sampled at large VZ angles. Sampling characteristics from MODIS are different with possible latitudinal dependency of REL AZM and solar zenith angle. Thus, careful categorization of the data will be undertaken prior to final analyses of the angular dependencies of the derived cloud properties.

4.2.3.3 Comparison with “cloud truth” datasets

To quantify the uncertainties and to better determine which set of angular conditions produce the most accurate vertical cloud structure, it necessary to compare the observations with other measurements that can be assumed to constitute cloud truth. Active remote sensors like lidar and radar can provide detailed information about cloud boundaries (e.g. Platt et al. 1980; Sassen et al. 1990; Miller and Albrecht 1995; Uttal et al. 1995). Such comparisons must be conducted carefully because of significant spatial and temporal differences between the various observing systems. For instance, it is important to account for the relatively small size of the lidar or radar field-of-view

(FOV), as compared to the much larger satellite FOV. Also, lidars and radars may retrieve different cloud boundaries, depending upon their sensitivity to cloud effective particle size, optical depth, etc. Comparisons of active remote sensor retrievals of cloud height have been used for a number of years to assess passive satellite estimates (e.g., Minnis et al. 1992; Minnis et al. 1993; Smith et al. 1996, 1997; Doelling et al. 1996; Minnis et al. 2000b). Differences between remotely-sensed and ground-based estimates of cloud cover must be examined carefully without automatically assuming that only one value is correct. The impact of multiple layering should also be considered to help explain differences and to justify excursions from desired accuracies. Because the CERES algorithms may derive cloud heights with several different algorithms, it will be necessary to evaluate all of those used in a given version for application to a specific imager. The results may allow future development to include logic that selects the best method for a particular set of conditions.

4.2.3.3.1 ARM sites

The highest priority set of observations will be those where CERES cloud properties can be compared *routinely* to those obtained at a well-known surface site such as that provided by the Atmospheric Radiation Measurement program. Extended observations will be provided by the ARM sites, but not at all the locations required according to the categories listed above. These include the Southern Great Plains site (central Oklahoma), the Tropical West Pacific sites, and the Arctic site (north slope of Alaska). The exact locations of these and other sites are listed in Minnis et al. (2000a). The CERES results can be compared to data from these sites over all seasons for a long time period in different cloud regimes. Cloud base can be measured several different ways at these sites using laser ceilometers, radar, and lidar. Cloud-top heights and layering can be assessed, primarily, with cloud radar measurements, but occasionally with lidar returns when the clouds are optically thin. Thus, in some cases a range of measurements can be used to assess the uncertainties in the surface observations relative to the satellite-derived values. The satellite imagery will be examined to help explain large differences in altitudes. Rawinsonde data are also available at the ARM sites, so that the radar-derived cloud heights will be converted to cloud-top temperature and compared directly to the corresponding satellite values. In that manner, it will be possible to determine if errors in the ECMWF soundings are a source of uncertainty in the derived cloud heights.

Figure 4 is an example of the comparisons that are being and will be performed over the ARM sites. It shows CERES effective cloud height and temperature matched with the cloud mean (center) and top heights and temperatures. This example includes all single-layer clouds over the ARM SGP site that occurred at the time of the daytime VIRS overpasses between January and July 1998 and had an optical depth τ less than 5. The CERES effective cloud temperature and height are the primary retrieved quantities. The remotely sensed cloud temperature corresponds to the effective radiating temperature of the cloud. If the top of the cloud is optically dense, then the effective temperature is near the cloud top. If the cloud top is diffuse, the particles are not densely concentrated, and the entire cloud is optically thin, then the effective temperature should correspond more closely to some location near the center of the cloud. For CERES, the cloud-top and base heights are derived from the effective quantities. For optically thick, low clouds, the effective height is assumed to be the same as the cloud-top height. For high ice clouds, cloud-top height depends on the optical depth and temperature. Cloud base height is determined from the cloud-top height and thickness. The latter quantity depends on the cloud temperature and phase. The quantities in Figure 4 were derived in the manner used by Dong et al. (1999). Except for two cases,

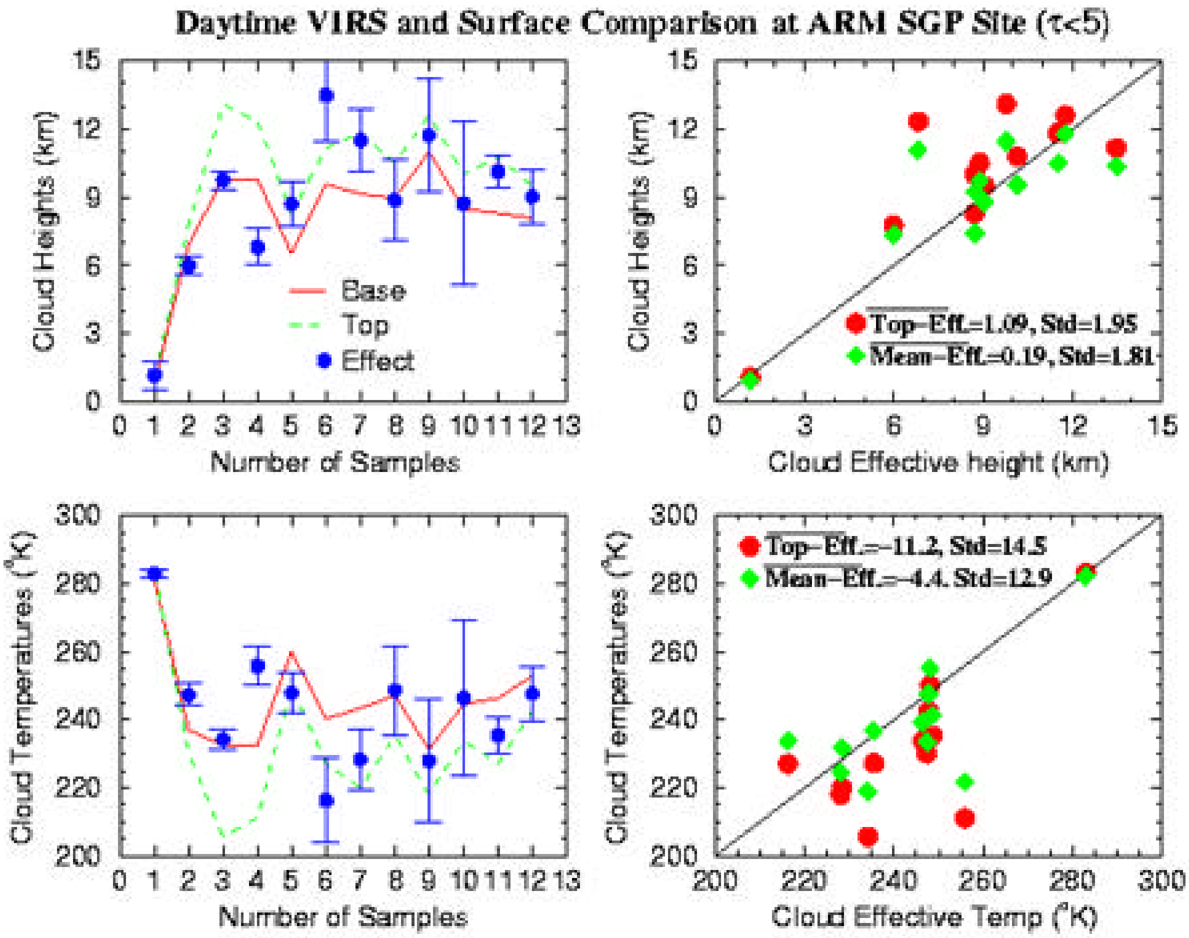

Figure 4. Comparison of surface-based cloud altitude (radar and ceilometer) and temperature (rawinsonde) boundaries with effective cloud height and temperature from VIRS derived with the CERES VISST for single-layer thin clouds over the ARM SGP site between January and July 1998.

the effective cloud center height and temperatures lie between the cloud top and base (left side of Figure 4). The actual cloud top and the effective height differ by 1.1 km, on average, with a 2-km standard deviation. The mean cloud effective heights are only 0.2 lower than the surface-derived mean cloud height confirming the assumed behavior of optically thin clouds noted above. Similar results were found for the nighttime algorithm except that the effective cloud heights were, on average, 0.3 km higher than the mean cloud height suggesting a relative height difference of 0.5 km between day and night. Thus, a purely infrared approach appears to yield lower optical depths and higher clouds relative to a visible-infrared technique and may cause some of the day-night differences in Figure 2. But it is not entirely clear if the cloud properties sampled for the nighttime cases are the same as those sampled during the daytime. Resolution of such discrepancies is part of the validation process.

An example of thick cloud height validation is shown in Figure 5. The same parameters are plotted except that all of the thick, single-layer clouds were used in this comparison. Here, the effective cloud height is only 0.4 km below the radar-derived cloud top and all but three of the effective cloud heights are within the radar-ceilometer derived cloud boundaries. The cloud tem-

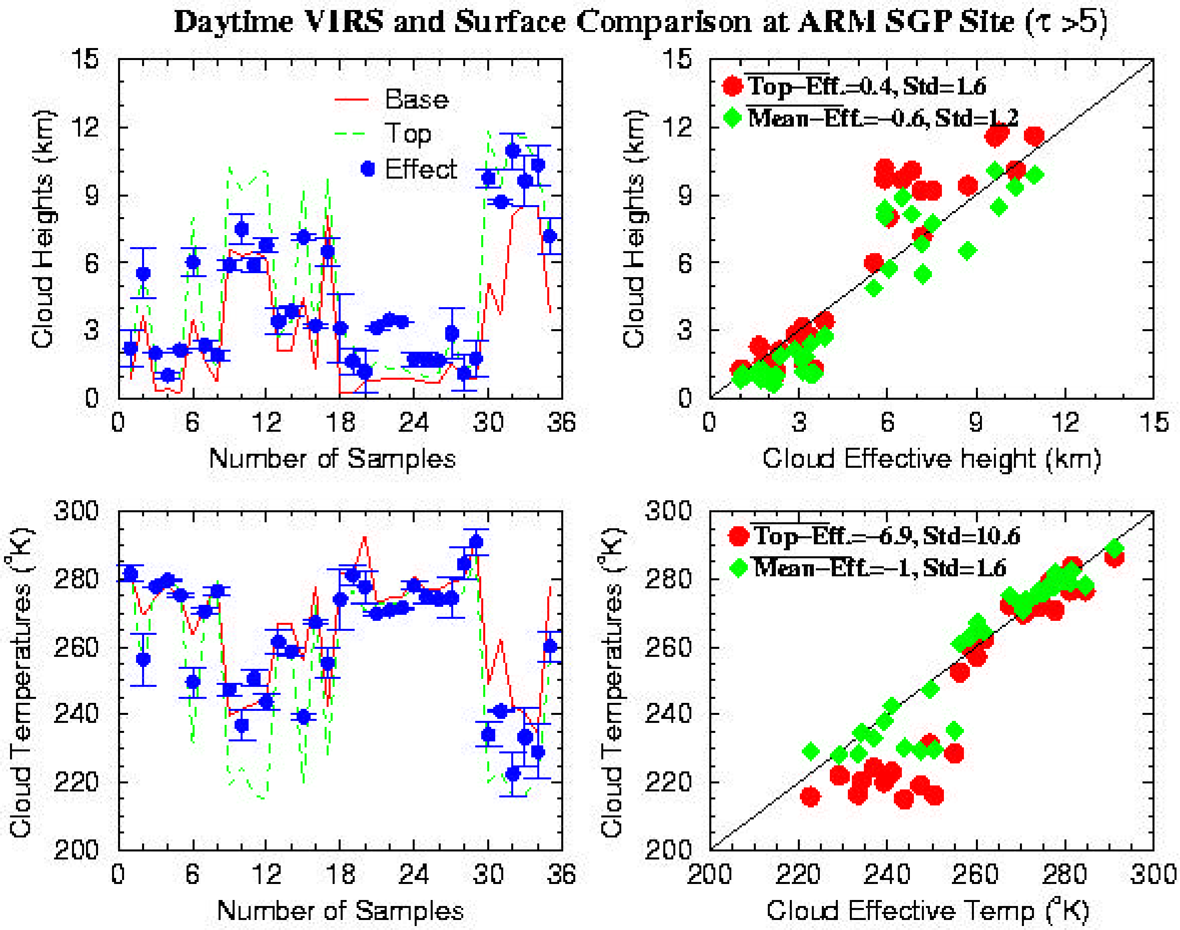

Figure 5. Comparison of surface-based cloud altitude (radar and ceilometer) and temperature (rawinsonde) boundaries with effective cloud height and temperature from VIRS derived with the CERES VISST for single-layer thick clouds over the ARM SGP site between January and July 1998.

peratures for those three cases, however, are the same from both the surface and the satellite indicating a problem with the ECMWF soundings. Another point of interest is that the effective height for the low clouds is equal to the cloud-top height as assumed in the CERES algorithm, but the effective height for the cirrus clouds varies from 0 to 4 km less than the cloud-top indicating that even for optically thick cirrus clouds, the cloud top is often diffuse and the radiating center is generally not close to the top. The results for the nighttime thick cloud cases are similar.

The above examples are just the first step in comparing the CERES cloud heights with cloud truth values derived from ARM active sensors. In addition to more detailed studies that compare CERES estimates of actual cloud top and base with the surface data, the occurrence and effects of multilayer cloud heights will also be examined and quantified. Data from the ARM sites will provide validation samples continuously for all seasons, for the local background conditions at each site. Researchers from the Terra validation program and the CERES Cloud Working Group will be responsible for acquiring, analyzing, and comparing the surface and CERES cloud height datasets.

4.2.3.3.2 Other routine surface observations

Active remote sensors are being used routinely or in a semi-operational fashion at other locations. Dr. Ken Sassen operates a set of lidars at the University of Utah in Salt Lake City. Data are taken when cirrus and a Terra overpass coincide. Dr. Robert Kropfli (NOAA/ETL) monitors clouds over Erie, Colorado (northeast of Denver) on a semi-operational basis between field programs with a suite sensors including a lidar and cloud radar. The Automated Surface Observing System (ASOS, Schreiner et al. 1993) over the continental United States includes ceilometer measurements. This network can be used only for validation of cloud-base heights for low clouds because the ceilometers generally have a detection limit of 4 km AGL. The CERES Cloud Working Group will obtain as many of these correlative data as possible to verify the cloud-top heights and bases over a wider range of backgrounds

4.2.3.3.3 Regional (short-term) comparison of CERES with ground-based observations

Field programs involving clouds often include cloud radars and/or lidars and are conducted in remote areas. Past (e.g., FIRE, SHEBA, ASTEX, ECLIPS, MCTEX, NAURU99, and TARFOX) and future field experiments (INCA, SAFARI, CRYSTAL, CLAMS, and others) will provide important validation data for their particular climatic and background conditions; however, validation samples over mid-latitude mountains, deserts, and tropical land should be included in future experiments. For pre-launch experiments, the exact VIRS and MODIS channels (spectra and resolution) were unavailable for comparison. Thus, the algorithms were tested using surrogate satellite (AVHRR, GOES, ATSR-2, etc.) data in those cases. For post-launch experiments, the VIRS and MODIS data as well as the surrogate imagers are used in the validation comparisons to distinguish between the results from each of the imaging systems so that the prelaunch results may be interpreted relative tot he expected performance of VIRS and MODIS.

The surface observations taken during the above field experiments are often similar to those taken regularly at the ARM sites. Thus, the same types of comparisons will be conducted for satellite overpasses to obtain the cloud height validations in areas where long-term observations are unavailable. Additionally, aircraft, like the NASA ER-2, with active remote sensors often fly during these experiments increasing the number of opportunities to collect some independent samples of clouds over remote areas. Every effort should be made in future experiments to align the flight times with the CERES satellite overpasses.

4.2.3.2 Operational surface networks

The following products are to be used in the validation activities:

a. National Weather Service (NWS) global synoptic cloud observations

b. DOE ARM data

c. Automated Surface Observing System (ASOS), installed on the National Environmental Satellite Data and Information Service VAS data utilization center in Washington, D.C.

4.2.3.3 Existing satellite data

A list of the satellite data sets used in pre-launch activities are:

1. AVHRR
2. HIRS
3. GOES-8, 9, 10
4. ISCCP cloud climatologies
5. HIRS cloud climatologies
6. ATSR-2

4.2.4 Additional Post-launch Activities

4.2.4.1 Planned field experiments and studies

The same approach as presented in Section 4.2.3.3 will be followed for additional post-launch activities. Cloud retrieval properties are not saved for all areas at the imager pixel level. Data from only a select set of regions are retained for validation. Additional pixel-level data will be archived whenever a relevant field program is conducted outside of the standard cloud validation regions (see Table 2, Minnis et al. 2000a). The subsetted data sets are produced by the Langley DAAC and provided to the CERES Cloud Working Group and other CERES Co-Investigators.

4.2.4.2 New EOS-targeted coordinated field campaigns

Even with the comparison of satellite to ground-based observations of cloud boundaries according to the strategies previously outlined, deficiencies will still exist over midlatitude oceans, mountains, deserts, and tropical land. To fill data-sparse gaps in our sampling, it would be beneficial to plan field campaigns for these areas.

4.2.4.3 Needs for other satellite data

To supplement the validation of cloud height and layering, in particular, the detection of multilayer clouds, it is desirable to develop liquid water path and temperature datasets over marine areas from the TRMM for matching the VIRS. Comparisons of the resulting cloud temperatures and the multilayer classifications like those indicated from the analyses of Lin et al. (1998) will be extremely useful for understanding the impact of multilayer conditions on the retrieved cloud properties over many areas for systems comprised of both thick and thin high-altitude ice clouds.

Another very useful set of satellite measurements for validation purposes would be lidar/radar observations, such as PICCASSO-CENA and CloudSat. The former will have a cloud and aerosol detecting lidar, while the latter will carry a cloud-detecting radar. These satellites are scheduled for launch in 2002 and will fly in tandem with one of the EOS satellites. Data from the other satellites used in the pre-launch validation should also be used for comparisons with the EOS results.

The vertical cloud structure will be defined quite accurately over all regions (swaths only a few hundred meters wide) at some time over the course of the satellites' lifetimes. Thus, the sampling needs for a reliable estimate of uncertainty in cloud-top height will be realized when these satellites become operational.

4.2.4.4 In-situ measurement needs at calibration/validation sites

The ideal set of instruments at the surface sites include a cloud lidar, a cloud radar, a laser ceilometer, and regular radiosonde launches. At present, the ARM sites have the most comprehensive set of instruments in this list.

4.2.4.5 Intercomparisons (multi-instrument)

Cloud-base heights from the ceilometer, lidar, and radar systems should be compared to estimate the uncertainty in these validation sets. Similarly, cloud heights measured with collocated VIRS and MODIS data should be compared to determine the robustness of the algorithms, verify angular dependence derived from one satellite, and to determine the effects of satellite resolution on the derived values. Additional experiments should be conducted to determine the optimal approach for comparing radar and satellite data to account for the spatial temporal mismatches in the two datasets.

4.2.5 Implementation of validation results in data production

4.2.5.1 Approach

The validation of cloud properties will take place at the CERES SCF and at the outside investigators' home institutions. While some of the global mapping functionality can be automated, most of the effort described in this document requires interaction with an investigator. The investigator will need ready access to cloud boundary information from each of the ARM sites or other sites that are operationally providing cloud boundary information, as well as access to the subsetted data sets of retrieved cloud properties.

4.2.5.2 Archival of validation data

The retrieved cloud parameters listed in Table 4.4-4 of CERES Subsystem 4.4, entitled "Convolution of imager cloud properties with CERES footprint point spread function", the volume of one hour of processed imager data is approximately 600 MB. These retrievals are not a product, but are subsequently convolved with CERES footprints to give a combined radiation-cloud-property product. The swaths (e.g., Figure 1) including the cloud validation regions (see Table 2 of Minnis et al. 2000a) and 351 1° x 1° CERES (all working groups) validation regions constitute the only pixel-level cloud parameter data saved by CERES. These validation datasets are produced and archived by the Langley DAAC.

4.2.6 References

Baum, B. A., P. Minnis, J. A. Coakley, Jr., B. A. Wielicki, and co-authors, 1995a: Imager cloud height determination (Subsystem 4.2). “Clouds and the Earth’s Radiant Energy System (CERES) Algorithm Theoretical Basis Document, Volume III: Cloud Analyses and Radiance Inversions (Subsystem 4)”, *NASA RP 1376 Vol. 3,* edited by CERES Science Team, 83-134.

Doelling, D. R.; Minnis, P.; Palikonda, R.; Ayers, J. K.; Ackerman, T. P.; Spinhirne, J. D.; and Platt, C. M. R., 1996: Validation of Satellite-Derived Cloud Properties During TOGA/ COARE. *12th International Conference on Clouds and Precipitation Proceedings - Volume 2*, Zurich, Switzerland, Aug. 19-23, 1281-1284.

Dong, X., P. Minnis, G. G. Mace, E. E. Clothiaux, C. Long, and S. Sun-Mack, 1999: Validation of CERES/VIRS cloud properties using ground-based measurements obtained at the DOE ARM sites. *Proc. AMS 10th Conf. Atmos. Rad.*, Madison, WI, June 28 – July 2, 29-32.

Heck, P. W.; Smith, W. L., Jr.; Minnis, P. and Young, D. F., Multispectral Retrieval of Nighttime Cloud Properties for CERES, ARM, and FIRE. *Proc. ALPS 99 Conference*, Meribel, France, January 18-22, 1999, **WK-P-03**,1,4.

Lin, B., P. Minnis, B. A. Wielicki, D. R. Doelling, R. Palikonda, D. F. Young, and T. Uttal, 1998: Estimation of water cloud properties from satellite microwave and optical measurements in oceanic environments. II: Results. *J. Geophys. Res.*, **103**, 3887-3905.

Miller, M. A. and B. A. Albrecht, 1995: Surface-based observations of mesoscale cumulus-stratocumulus interaction during ASTEX. *J. Atmos. Sci.*, **52**, 2809-2826.

Minnis, P., D. R. Doelling, V. Chakrapani, D. A. Spangenberg, T. Uttal, R. F. Arduini, and M. Shupe, 2000b: Cloud coverage during FIRE ACE derived from AVHRR data. In press, *J. Geophys. Res.*, August.

Minnis, P., P. W. Heck, and D. F. Young, 1993: Inference of cirrus cloud properties using satellite-observed visible and infrared radiances, Part II: Verification of theoretical cirrus radiative properties. *J. Atmos. Sci.*, **50**, 1305-1322.

Minnis, P., P. W. Heck, D. F. Young, C. W. Fairall, and J. B. Snider, 1992: Stratocumulus cloud properties derived from simultaneous satellite and island-based instrumentation during FIRE, *J. Appl. Meteor.*, **31**, 317-339.

Minnis, P.; Kratz, D. P.; Coakley, J. A., Jr.; King, M. D.; Garber, D.; Heck, P.; Mayor, S.; Young, D. F. and Arduini, R., 1995: Cloud Optical Property Retrieval (Subsystem 4.3). "Clouds and the Earth's Radiant Energy System (CERES) Algorithm Theoretical Basis Document, Volume III: Cloud Analyses and Radiance Inversions (Subsystem 4)", *NASA RP 1376 Vol. 3*, edited by CERES Science Team, December, 135-176.

Minnis, P., L. Nguyen, D. F. Young, R. M. Welch, and B. A. Baum, 2000a: Clouds and the Earth’s Radiant Energy System (CERES) Validation Document, Imager Clear-sky Determination and Cloud Detection (Subsystem 4.1). Intenal document available on the World Wide Web at http://asd-www.larc.nasa.gov/ceres/ASDceres.html.

Minnis, P., W. L. Smith, Jr., D. F. Young, and P. W. Heck, 1993: Cloud fields derived from satellite and surface data during FIRE Cirrus Phase II. *Proc. FIRE Cirrus Science Conf.*, Breckenridge, CO, June 14-17, 36-39.

Minnis, P., Young, D. F., Spangenberg, D. A., Heck, P. W., D. R. Doelling, Q. Trepte, and Y. Chen, 1999a: Cloud mask for CERES from VIRS on the TRMM satellite. *Proc. ALPS 99 Confer-*

ence, Meribel, France, January 18-22, **WK-P-06**, 1-4.

Minnis, P., D. F. Young, B. A. Wielicki, P. W. Heck, X. Dong, L. L. Stowe, R. Welch, 1999b: CERES cloud properties derived from multispectral VIRS data. *Proc. The EOS/SPIE Symposium on Remote Sensing*, **Vol. 3867**, Florence, Italy, September 20-24, 91-102.

Minnis, P., D. F. Young, B. A. Wielicki, P. W. Heck, S. Sun-Mack, and T. D. Murray, 1999a. Cloud properties derived from VIRS for CERES. *Proc. AMS 10th Conf. Atmos. Rad.*, Madison, WI, June 28 – July 2, 21-24.

Platt, C. M. R., D. W. Reynolds, and N. L. Abshire, 1980: Satellite and lidar observations of the albedo, emittance and optical depth of cirrus compared to model calculations. *Mon. Wea. Rev.*, **108**, 195-204.

Sassen, K., C. J. Grund, J. Spinhirne, M. Hardesty and J. M. Alvarez, 1990: The 27-28 October 1986 FIRE IFO cirrus case study: A five lidar overview of cloud structure and evolution. *Mon. Wea. Rev.*, **118**, 2288-2311.

Schreiner, A. J., D. A. Unger, W. P. Menzel, G. P. Ellrod, K. I. Strabala, and J. L. Pellet, 1993: A comparison of ground and satellite observations of cloud cover. *Bull. Amer. Meteor. Soc.*, **74**, 1851-1861.

Smith, W. L., Jr.; L. Nguyen, D. P. Garber, D. F. Young, P. Minnis, and J. Spinhirne: Comparisons of Cloud Heights Derived From Satellite and ARM Surface Lidar Data, 1997: Proceedings of 6th Annual ARM Science Team Meeting, San Antonio, Texas, March 4-7, 1996, 287-291.

Smith, W. L., Jr.; Nguyen, L.; Garber, D. P.; Minnis, P.; Young, D. F.; Winker, D.; McCormick, M. P.; Smith, W. L.; and Huang, H. L.: Comparisons of Cloud Heights Derived from Satellite, Aircraft, Surface Lidar, and LITE Data. 1996 International Radiation Symposium, Fairbanks, Alaska, August 19-23, 1996, 603-606.

Uttal, T. E. E. Clothiaux, T. P. Ackerman, J. M. Intrieri, and W. L. Eberhard, 1995: Cloud boundary statistics during FIRE II, *J. Atmos. Sci.*, **52**, No. 23, 4276-4284.

4.2.7 List of Acronyms

ARM	Atmospheric Radiation Measurement Program
ASTEX	Atlantic Stratocumulus Transition Experiment
ATSR-2	Along-Track Scanning Radiometer
AVHRR	Advanced Very High Resolution Radiometer
CENA	Climatologie Etendue des Nuages et des Aerosols
CERES	Cloud’s and the Earth’s Radiant Energy System
CLAMS	Chesapeake Lighthouse and Aircraft Measurements for Satellites
CRYSTAL	Cirrus Regional Study of Tropical Anvils and Cirrus Layers
DAAC	Distributed Active Archive Center
DOE	Department of Energy
ECLIPS	Experimental Cloud Lidar Pilot Study
ECMWF	European Center for Medium Range Weather Forecasting
FIRE	First ISCCP Regional Experiment
GOES	Geostationary Operational Environmental Satellite
HIRS	High-resolution Infrared Radiometer Sounder

INCA	INterhemispheric differences in Cirrus properties from Anthropogenic emissions
ISCCP	International Satellite Cloud Climatology Experiment
LITE	Lidar in Space Technology Experiment
LBTM	Layer Bispectral Threshold Method
MODIS	Moderate resolution Imaging Spectrometer
NAURU99	Nauru Island ARM Experiment in 1999
NMC	National Meteorological Center
PICASSO	Pathfinder Instruments for Cloud and Aerosol Spacebourne Observations
SAFARI	South African Regional Science Initiative
SCF	Southern Great Plains Central Facility
SHEBA	Surface HEat Budget in the Arctic
SIST	Solar-infrared Infrared Split-window Technique
TARFOX	Tropospheric Aerosol Radiative Forcing Observational Experiment
TRMM	Tropical Rainfall Measuring Mission
VIRS	Visible and Infrared Scanner
VISST	Visible Infrared Solar-infrared Split-window Technique

SUMMARY OF CERES VALIDATION OF IMAGER CLOUD-TOP AND CLOUD BASE HEIGHTS

DATA PRODUCTS/PARAMETERS

- Parameters: Cloud-top and cloud-base heights for both single- and multiple-layered clouds

  Product: CERES SSF

MISSIONS

- TRMM, EOS AM-1, & EOS PM-1

APPROACH:

- First develop global and regional maps of retrieved cloud heights
- Show that global and regional analyses indicate consistent results moving from ocean to land, day to night, snow to water, desert to water, etc.
- Once results are consistent, compare retrieved cloud boundaries with ground-based, other satellite-based, or aircraft-based data of cloud boundaries (most appropriate for stratiform clouds)
- Comparisons of simultaneous retrievals from multiple satellites, aircraft and satellite, or surface with satellite

PRELAUNCH

- Compare cloud boundary data from field programs with satellite retrievals
- Compare surface synoptic observations with satellite retrievals of single and multilevel cloud occurrences

SUMMARY OF CERES VALIDATION OF IMAGER CLOUD-TOP AND CLOUD BASE HEIGHTS

POSTLAUNCH

- Increase number of long-term monitoring sites to include midlatitude oceans, mountains, deserts, and tropical land
- Develop field programs over surface types where little if any data currently exist, such as deserts
- Perform quick-look global and regional analyses of cloud boundary products
- Compare CERES cloud boundary retrievals with validation sites

EOSDIS

- Perform subsetting of processed full-resolution CERES imager data stream
- Archive validation site cloud boundary data